Van der Waals Attraction of Vortices in Anisotropic and Layered Superconductors

Gianni Blatter[1] and Vadim Geshkenbein[1,2]
[1]*Theoretische Physik, ETH-Hönggerberg, CH-8093 Zürich, Switzerland*
[2]*L. D. Landau Institute for Theoretical Physics, 117940 Moscow, Russia*
(Received 12 July 1996)

We show that in anisotropic and layered superconductors the fluctuations of vortex lines produce an attractive long-range vortex-vortex interaction of the van der Waals type. This attraction follows from the anisotropic screening properties of the material and has profound consequences for the low-field phase diagram of these materials. [S0031-9007(96)01803-0]

PACS numbers: 74.60.Ec, 74.60.Ge

It is general knowledge that vortices in type II superconductors repel one another on all scales [1]. The repulsion follows a logarithmic law on distances $r < \lambda$ and decays exponentially on scales $r > \lambda$, where λ denotes the magnetic penetration depth. This result remains true in the presence of thermal (or quantum) fluctuations of the vortex lines as long as the material is isotropic. In an anisotropic or layered material, however, fluctuations produce an attractive long-range interaction beyond the scale λ. This long-range attraction is of the van der Waals type and leads to a variety of interesting novel phenomena in dilute vortex systems. In this Letter, we derive the van der Waals type attractive force between vortices in anisotropic and layered superconductors and investigate the phase diagram of the dilute vortex system, comprising a first-order transition at H_{c_1} and new generic van der Waals vortex solids and liquids. The work has been inspired by the study of Brandt, Mints, and Snapiro [2] of the fluctuation-induced attraction of vortices to surfaces.

The occurrence of a van der Waals type attractive force between vortex lines is most simply illustrated in an extremely layered superconductor with no superconducting coupling between the layers: Consider two straight vortices 1 and 2 at a distance R. Displacing an individual pancake vortex in the stack 1 by u_1 is equivalent to placing a pancake–antipancake pair, i.e., a pancake dipole d_1, onto the vortex line. The pancake dipole d_1 induces a second dipole d_2 in vortex 2 within the same layer. With two pancakes interacting logarithmically within the same layer, the force from dipole d_1 acting on vortex 2 follows a $1/R^2$ law, hence $d_2 \propto d_1/R^2$. Finally, the interaction potential between two vortex dipoles follows a $1/R^2$ behavior as well and we obtain a long-range attractive potential $V_{\mathrm{vdW}} \propto 1/R^4$ between the vortex segments. The initial fluctuation d_1 can be induced thermally or, at low temperatures, quantum mechanically.

In an anisotropic material the same mechanism is at work with slight modifications. Crucial for the understanding of the effect are the different screening properties of the material parallel and perpendicular to the axis of anisotropy, the c axis. Let $\varepsilon^2 = m/M \ll 1$ denote the anisotropy of the material, with m and M the effective masses parallel and perpendicular to the ab plane. The anisotropy parameter ε quantifies the Josephson coupling between the layers of the anisotropic material. Whereas currents flowing within the ab planes are screened on a scale λ, the out-of-plane currents decay only on the longer scale λ/ε. Placing two vortices parallel to the c axis at a distance R, a fluctuation in vortex 1 again induces a "counterfluctuation" in vortex 2 with the transverse parts of the vortex lines attracting one another within the distance $R < \lambda/\varepsilon$. Within the range $\lambda < R < d/\varepsilon$ (d denotes the layer separation), the Josephson coupling is irrelevant and the van der Waals interaction follows the behavior of the uncoupled system, $V_{\mathrm{vdW}} \propto 1/R^4$. At larger distances $d/\varepsilon < R < \lambda/\varepsilon$, the c-axis currents are relevant and the interaction drops faster, $V_{\mathrm{vdW}} \propto 1/R^5$. For strong coupling with $d/\varepsilon < \lambda$, only the latter regime survives.

It is quite instructive to compare the van der Waals attraction between vortices in anisotropic superconductors with the fluctuation-induced attraction between neutral atoms. The latter decays on short distances with the famous $1/r^6$ power law, turning into a $1/r^7$ behavior at large distances when retardation effects come into play [3]. The changeover from a $1/R^4$ to a $1/R^5$ behavior in the vortex system is an analogous effect. This can be most simply understood when the vortex problem is mapped onto the imaginary time quantum problem of charged bosons, see Refs. [4] and [5]. The vortex-vortex interaction then turns into a nonlocal in time interaction between the bosons, and the $1/R^5$ behavior is a consequence of the corresponding retardation effects. Whereas the usual van der Waals interaction between atoms is due to (longitudinal) electric dipole fluctuations, in the vortex problem the interaction is of a transverse nature with current fluctuations generating the force. Such a transverse van der Waals force also exists for the atomic problem; however, it involves the small parameter v^2/c^2. In the charged boson problem the effective velocity of light is smaller, and the corresponding velocity ratio squared is of the order of the two-dimensional (2D) Ginzburg number. In the following we determine the van der Waals force between two vortices and then discuss the low-field phase diagram in layered superconductors.

 0031-9007/96/77(24)/4958(4)$10.00

Consider two parallel flux lines directed along the z axis and separated by a distance R. Within the London approximation, the functional $\mathcal{F}$ providing the configurational energy of the two vortices takes the form [5]

$$\mathcal{F}[\mathbf{s}_\mu] = \sum_{\mu,\nu=1}^{2} \frac{\varepsilon_\circ}{2} \int ds_{\mu\alpha} ds_{\nu\beta}\, V^{\rm int}_{\alpha\beta}(\mathbf{s}_\mu - \mathbf{s}_\nu). \quad (1)$$

Here, $\mathbf{s}_\mu = \mathbf{r}_\mu + \mathbf{u}_\mu(z)$, $\mu = 1, 2$, denote the positions of the two vortices, with $\mathbf{u}_\mu(z)$ the fluctuating part, $\varepsilon_\circ = (\Phi_\circ/4\pi\lambda)^2$ the basic energy scale, and $V^{\rm int}_{\alpha\beta}$ the interaction between two vortex segments, for an isotropic material $V^{\rm int}_{\alpha\beta}(r) = \delta_{\alpha\beta}\exp(-r/\lambda)/r$. In a uniaxially anisotropic material with the crystal axis $\mathbf{c} \parallel \hat{\mathbf{z}}$, the interaction is conveniently expressed through its Fourier representation,

$$V^{\rm int}_{\alpha\beta}(\mathbf{r}) = 4\pi\lambda^2 \int \frac{d^3k}{(2\pi)^3}\, e^{i\mathbf{kr}} V^{\rm int}_{\alpha\beta}(\mathbf{k}), \quad (2)$$

$$V^{\rm int}_{\alpha\beta}(\mathbf{k}) = \frac{e^{-(\xi^2K^2+\xi_c^2k_z^2)}}{1 + \lambda^2k^2} \times \left[\delta_{\alpha\beta} - \frac{(\lambda_c^2 - \lambda^2)K_{\perp\alpha}K_{\perp\beta}}{1 + \lambda^2k^2 + (\lambda_c^2 - \lambda^2)K^2}\right]. \quad (3)$$

Here, $\mathbf{K} = (k_x, k_y)$ and $\mathbf{K}_\perp = (k_y, -k_x)$. We choose $\mathbf{r}_1 = (\mathbf{R}, z_1)$, $\mathbf{r}_2 = (0, 0, z_2)$, and define $d\mathbf{s} = \mathbf{t}dz$ with the tangential vector $\mathbf{t} = [\partial_z\mathbf{u}(z), 1]$. The energy is split into the self-energy part $\mathcal{F}_0$ with $\mu = \nu$, and an interaction part $\mathcal{F}_{\rm int}$ with $\mu \neq \nu$,

$$\mathcal{F}_{\rm int} = \frac{\Phi_\circ^2}{4\pi} \int \frac{d^3k}{(2\pi)^3}\, dz_1 dz_2 \times [V^{\rm int}_{zz}(\mathbf{k}) + t_{1\alpha}(z_1)t_{2\beta}(z_2)V^{\rm int}_{\alpha\beta}(\mathbf{k})] \times e^{i\mathbf{K}[\mathbf{R}+\mathbf{u}_1(z_1)-\mathbf{u}_2(z_2)]}e^{ik_z(z_1-z_2)}. \quad (4)$$

We determine the interaction between the vortices using conventional statistical mechanics techniques to account for the fluctuations. With the partition function,

$$Z(R) = \int \mathcal{D}[\mathbf{u}_1(z)]\mathcal{D}[\mathbf{u}_2(z)] \exp[-\mathcal{F}(R)/T], \quad (5)$$

the free energy takes the form (up to a constant)

$$F(R) = -T\ln Z(R) = -T\ln\langle\exp[-\mathcal{F}_{\rm int}(R)/T]\rangle_0, \quad (6)$$

where the average $\langle\cdots\rangle_0$ is taken with the self-energy term $\mathcal{F}_0$ describing the noninteracting vortices. Performing a cumulant expansion in (6) the expression for the effective vortex-vortex interaction takes the form

$$LV_{\rm eff}(R) \approx \langle\mathcal{F}_{\rm int}\rangle_0 - [\langle\mathcal{F}_{\rm int}^2\rangle_0 - \langle\mathcal{F}_{\rm int}\rangle_0^2]/2T. \quad (7)$$

Here, L denotes the sample dimension along the field direction. We split the interaction into a longitudinal term $\mathcal{F}_\parallel$ [involving the term V_{zz} in Eq. (4)] and a transverse part $\mathcal{F}_\perp$ [$t_{1\alpha}t_{2\beta}V_{\alpha\beta}$ in Eq. (4)], $\mathcal{F}_{\rm int} = \mathcal{F}_\parallel + \mathcal{F}_\perp$. To lowest order in $\mathbf{u}_\mu$ the term $\langle\mathcal{F}_\parallel\rangle_0$ provides the usual mean-field-type expression for the vortex-vortex interaction,

$$V^{(0)}_{\rm eff}(R) = 2\varepsilon_\circ K_0(R/\lambda), \quad (8)$$

with K_0 the zero-order modified Bessel function. Higher order expansions in $\mathbf{u}_\mu$ only renormalize the prefactor but do not change the form of the interaction. The transverse term $\langle\mathcal{F}_\perp\rangle_0$ vanishes, except for the situation where the vortex is close to a surface $\parallel z$; in this latter case this first-order term describes the van der Waals type long-range attraction of the vortex to the surface [2]. We will comment below in more detail on this situation.

The second-order term in $\mathcal{F}_\parallel$ again renormalizes the repulsive interaction between the vortices but does not produce a long-range component. On the contrary, the term $\langle\mathcal{F}_\perp^2\rangle_0$ produces a long-range attraction between the vortices, thus providing the van der Waals potential

$$V_{\rm vdW}(R) = -\frac{\langle\mathcal{F}_\perp\mathcal{F}_\perp\rangle_0}{2TL}. \quad (9)$$

To lowest order in the displacements,

$$\mathcal{F}_\perp = \frac{\Phi_\circ^2}{4\pi} \int \frac{d^3k}{(2\pi)^3}\, t_{1\alpha}(-k_z)t_{2\beta}(k_z)V^{\rm int}_{\alpha\beta}(\mathbf{k})e^{i\mathbf{KR}}, \quad (10)$$

$$\langle\mathcal{F}_\perp\mathcal{F}_\perp\rangle_0 = \frac{\Phi_\circ^4 L}{64\pi^2} \int \frac{dk_z}{2\pi}[V^{\rm int}_{\alpha\beta}(\mathbf{R}, k_z)]^2\langle t^2(k_z)\rangle_0^2, \quad (11)$$

where we have defined the partial Fourier transform

$$V^{\rm int}_{\alpha\beta}(\mathbf{R}, k_z) = \int \frac{d^2K}{(2\pi)^2} V^{\rm int}_{\alpha\beta}(\mathbf{K}, k_z)e^{i\mathbf{KR}}, \quad (12)$$

and we have used $\langle t_{1\alpha}(-k_z)t_{2\beta}(k_z)t_{1\alpha'}(-k_z')t_{2\beta'}(k_z')\rangle_0 = 2\pi L\delta(k_z - k_z')\delta_{\alpha\alpha'}\delta_{\beta\beta'}\langle t^2(k_z)\rangle_0^2/4$.

We first concentrate on the decoupled limit $\varepsilon \to 0$. Using (3) in the limit $\varepsilon \to 0$, the partial Fourier transform (12) takes the form [we use $\mathbf{R} = (R > \lambda, 0)$]

$$V^{\rm int}_{xx}(R, k_z) = -\frac{1}{2\pi R^2}\frac{1}{1 + \lambda^2k_z^2} \approx -V^{\rm int}_{yy}(R, k_z), \quad (13)$$

where we have dropped a small correction $\propto\exp(-R/\lambda)$ in the second equation (the mixed terms $V^{\rm int}_{xy}$ and $V^{\rm int}_{yx}$ vanish). The single vortex fluctuation amplitude

$$\langle t^2(k_z)\rangle_0 = \frac{T}{\varepsilon_l(k_z)} \quad (14)$$

is determined by the line elasticity $\varepsilon_l(k_z)$; in the decoupled limit, $\varepsilon_l(k_z) = (\varepsilon_\circ/2\lambda^2k_z^2)\ln(1 + \lambda^2k_z^2)$, i.e., only the electromagnetic coupling producing a strongly dispersive line tension is relevant. Combining the above elements, we arrive at the final expression for the van der Waals potential in the *decoupled limit*,

$$V^{\rm dc}_{\rm vdW}(R) = -\frac{\varepsilon_\circ}{\ln^2(\lambda\pi/d)}\frac{T}{d\varepsilon_\circ}\left(\frac{\lambda}{R}\right)^4. \quad (15)$$

We turn to the continuous anisotropic case with $\varepsilon > 0$. The partial transform (12) now reads

$$V^{\rm int}_{xx} = \frac{(-1)}{2\pi R}\frac{\varepsilon}{\lambda\sqrt{1 + \lambda^2k_z^2}}K_1\left(\varepsilon R\sqrt{1 + \lambda^2k_z^2}/\lambda\right), \quad (16)$$

with K_1 the first-order modified Bessel function, $K_1(z \to 0) \sim 1/z$, $K_1(z > 1) \sim \sqrt{\pi/2z}\exp(-z)$. Again, $V^{\rm int}_{yy} \approx -V^{\rm int}_{xx}$ up to a small correction. Within the regime

$\lambda < R < d/\varepsilon$ the expression (16) reduces to (13), and the van der Waals potential remains unchanged. On the other hand, for $\lambda, d/\varepsilon < R$, the Bessel function K_1 cuts off the k_z integral at $1/\varepsilon R$, and we obtain the result for the *continuous anisotropic* case (see Ref. [6])

$$V_{\rm vdW} = \begin{cases} \dfrac{(-\varepsilon_\circ)}{\ln^2(\pi\lambda/d)}\,\dfrac{T}{d\varepsilon_\circ}\,\dfrac{\lambda^4}{R^4}, & \lambda < R < \dfrac{d}{\varepsilon}, \\ \dfrac{(-3\pi/32)\varepsilon_\circ}{\ln^2(\pi\lambda/\varepsilon R)}\,\dfrac{T}{\varepsilon\lambda\varepsilon_\circ}\,\dfrac{\lambda^5}{R^5}, & \lambda, \dfrac{d}{\varepsilon} < R < \dfrac{\lambda}{\varepsilon}. \end{cases} \tag{17}$$

The van der Waals attraction involves large k_z values and thus derives from distances $\delta z < d$ and $\delta z < \varepsilon R < \lambda$ on small ($\lambda < R < d/\varepsilon$) and large ($\lambda, d/\varepsilon < R$) vortex separations, respectively. Also note that, throughout the regime $k_z < 1/\varepsilon R < 1/\varepsilon\lambda$, the single vortex elasticity is dominated by the electromagnetic coupling.

We briefly discuss the van der Waals attraction of an individual vortex 1 to a parallel surface, which we choose to be the yz plane. The vortex 2 then represents the mirror image of vortex 1, and hence $\mathbf{r}_2 = (-R, 0, z_2)$, $\mathbf{u}_2 = (-u_{1x}, u_{1y})$. The van der Waals potential originates from the transverse interaction

$$\langle \mathcal{F}_\perp \rangle_0 = \frac{\Phi_\circ^2 L}{16\pi} \int \frac{dk_z}{2\pi} [V_{xx}^{\rm int} - V_{yy}^{\rm int}] \langle t^2(k_z)\rangle_0 \tag{18}$$

[we have used $\langle t_{1\alpha}(-k_z) t_{2\alpha}(k_z)\rangle_0 = \pm L\langle t^2(k_z)\rangle_0/2$ and have included a minus sign to account for the opposite circulation of the image vortex]. In the decoupled limit the van der Waals surface attraction takes the form

$$V_{\rm vdW}^{\rm s,dc}(R) = -\frac{\varepsilon_\circ}{\ln(\lambda\pi/d)}\,\frac{T}{d\varepsilon_\circ}\left(\frac{\lambda}{R}\right)^2, \tag{19}$$

where we have made use of (13). For finite coupling $\varepsilon > 0$ we use the partial transform (16) and arrive at

$$V_{\rm vdW}^{\rm s} = \frac{(-\varepsilon_\circ/2)}{\ln(\pi\lambda/\varepsilon R)}\,\frac{T}{\varepsilon\lambda\varepsilon_\circ}\,\frac{\lambda^3}{R^3}, \quad \lambda, \frac{d}{\varepsilon} < R < \frac{\lambda}{\varepsilon} \tag{20}$$

[for short distances $\lambda < R < d/\varepsilon$, the result (19) applies]. The results (19) and (20) differ from those obtained in Ref. [2], where no thermal van der Waals type vortex-surface attraction has been found. The origin of the discrepancy can be traced back to the different approaches taken in Ref. [2] and here: Whereas Brandt *et al.* determine the energy of the vortex as it approaches the surface, we derive the van der Waals potential from a calculation of the *free energy*. The entropic contribution to the free energy then produces a nonvanishing vortex-surface attraction.

The appearance of an attractive van der Waals type interaction between vortex lines has interesting consequences for the low-field ($B \sim$ a few Gauss) phase diagram of anisotropic/layered superconductors, see Fig. 1. With the external magnetic field H fixed, we have to analyze the Gibbs free energy density $G(H,T) = F(B,T) + B(H_{c_1}^\circ - H)/4\pi$, where $H_{c_1}^\circ = 4\pi\varepsilon_\circ \ln\kappa/\Phi_\circ$ is the unrenormalized lower critical field. The free energy density F is composed of an interaction term $(z/2)V_v(a_\circ)/a_\circ^2$ and an entropic contribution $-T[S_l - S_v(a_\circ)]/a_\circ^2$. Here, $a_\circ = \sqrt{\Phi_\circ/B}$ denotes the distance between the flux lines and z is the number of nearest neighbors, $z = 6$ in a triangular lattice. The vortex-vortex interaction V_v is the sum of the repulsive term $2\varepsilon_\circ K_0(a_\circ/\lambda)$ [see Eq. (8)] and the attractive van der Waals interaction $-2\varepsilon_\circ\gamma_v(\lambda/a_\circ)^5$ with $\gamma_v = [3\pi/64\ln^2(\pi\lambda/\varepsilon a_\circ)](T/\varepsilon\varepsilon_\circ\lambda)$ [see Eq. (17); this approximation underestimates the attraction in the dilute case]. The entropic term consists of an irrelevant single vortex contribution S_l, which does not depend on the vortex density and merely renormalizes the lower critical field $H_{c_1}^\circ \to H_{c_1}^r$. The second term $S_v(a_\circ)$ describes the *reduction* of the line entropy S_l due to the confinement of an individual vortex within the cage set up by its neighbors [4]. Making use of the equivalence between the statistical mechanics of lines and the quantum mechanics of 2D bosons [4], we have to calculate the binding

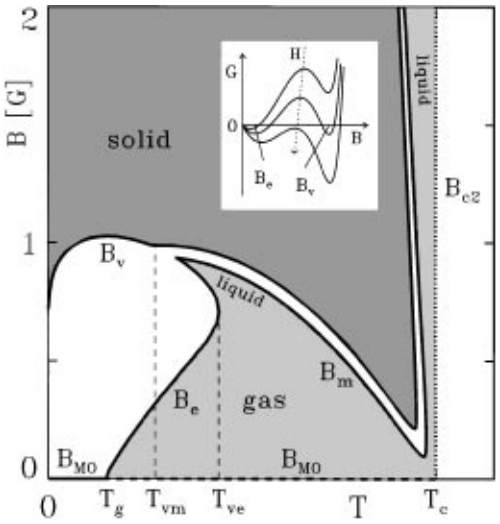

FIG. 1. Low-field phase diagram for a layered superconductor. Parameters appropriate for $Bi_2Sr_2Ca_1Cu_2O_8$ have been used ($\lambda = 1800$ Å, $\varepsilon = 1/300$, $c_L = 0.3$, see Ref. [7]). Continuous lines denote first-order transitions (note the associated jumps in B); the dashed line is a second-order transition. At low temperatures $T < T_g, T_{vm}$, the MO phase ($B_{\rm MO}$) becomes unstable towards a vortex solid ($B > B_v$) at $H_{c_1} < H_{c_1}^r$. At the temperature T_g a new vortex gas phase appears at low densities ($B < B_e$), rendering the MO phase unstable at $H_{c_1} > H_{c_1}^r$. At a higher magnetic field $H_{cv} > H_{c_1}$ a transition to a solid phase takes place ($B > B_v$). The latter melts at T_{vm}, giving way to a sliver of vortex liquid in the high-density region above B_v. At temperatures $T > T_{ve}$ larger than critical, we can no longer distinguish between the low-density vortex gas and the high-density vortex liquid regimes—we call the resulting phase a vortex gas. With increasing external field H this gas transforms into a vortex solid ($B > B_m$). With increasing anisotropy the critical temperatures T_g and T_{ve} move towards higher temperatures. The reentrant nose close to T_c is only a schematic drawing. The inset shows the free energy G versus induction B at fixed temperature $T > T_g$ for three values of the magnetic field H.

energy E_g of a particle in a circular hard-wall well and obtain the entropy reduction $TS_v(a_\circ) = E_g - V \rightarrow z_e(T^2/\varepsilon_\circ a_\circ^2)$, with $z_e = \pi x_{00}^2/2$, and $x_{00} \approx 2.405$ the first zero of the Bessel function J_0. Combining the above elements and introducing $x = a_\circ/\lambda$ as our dimensionless variable, we arrive at the following expression for the Gibbs free energy density:

$$G(x, H, T) = \frac{\varepsilon_\circ}{\lambda^2 x^2}\left[zK_0(x) - \frac{z\gamma_v}{x^5} + \frac{\gamma_e}{x^2} + \gamma_H \right], \tag{21}$$

with $\gamma_e = z_e(T/\varepsilon_\circ\lambda)^2$ and $\gamma_H = \ln(\lambda/\xi)\,(1 - H/H_{c_1}^r)$, ξ denoting the planar coherence length. In order to find the magnetic induction $B = \Phi_\circ/\lambda^2 x^2$ at given external parameters T and H, we have to minimize G with respect to B. The most general behavior of G versus B at fixed temperature T and for various fields H is shown in the inset of Fig. 1 ($T_g < T < T_{ve}$). The low-density minimum at B_e results from the competition between the entropic repulsion and the van der Waals attraction between the vortices. At the high-density minimum B_v the entropic repulsion has been overcome, and the van der Waals attraction is balanced by the hard core repulsion ($\propto K_0$) between the flux lines. The transition between the two phases takes place at $H = H_{cv}$ rendering $G|_{B_e} = G|_{B_v}$, while the densities are found from the conditions $\partial_B G|_{B_e,B_v} = 0$. Typical vortex separations in the high-density phase are of the order of $x_v \approx 20\lambda$. Reducing H below H_{cv}, the low-density minimum at B_e smoothly shifts towards smaller field values, and, finally, the Meissner-Ochsenfeld (MO) phase with $B_{\mathrm{MO}} = 0$ is stabilized at H_{c_1}, $H_{c_1}^r < H_{c_1} < H_{cv}$. Similarly, reducing the temperature T towards T_g, the low-density minimum at B_e approaches zero induction, such that at T_g the low-density phase is lost, with the MO and the dense vortex phase remaining the only two available phases. The temperature T_g is determined by the condition $G|_{B_v} = 0$, resulting in the expression $T_g^2 = (z/2z_e)a_g^2\varepsilon_\circ|V_v(a_g)|$ with $B_g = B_v(T_g)$. Furthermore, we have $H_{cv} = H_{c_1}^r$ at T_g. For low temperatures $T < T_g$ the surviving high-density phase is determined by the conditions $G|_{B_v} = G|_{B_{\mathrm{MO}}} = 0$ and $\partial_B G|_{B_v} = 0$. However, increasing the temperature towards T_{ve}, the low- and high-density phases approach one another and merge at the temperature T_{ve}, the latter being determined by the conditions $\partial_B G = \partial_B^2 G = \partial_B^3 G = 0$.

In order to complete our analysis we have to determine the stability of the vortex lattice with respect to thermal fluctuations. Within a Lindemann melting scenario we can easily determine the phase boundary $B_m(T)$ of the vortex solid [8]. When the mean squared fluctuations $\langle u^2\rangle = T/\sqrt{2\pi\varepsilon_\circ c_{66}}$ reach a fraction c_L^2 of the unit cell area $a_\circ^2$ the lattice becomes unstable and melts. In the low-field region considered here the melting transition is driven by the exponential decay of the shear modulus $c_{66} \propto \exp(-a_\circ/\lambda)$. The solid-liquid transition along the high-density phase line $B_v(T)$ can be determined from the condition $B_v(T_{vm}) = B_m(T_{vm}) = B_{vm}$, and results in a melting temperature

$$T_{vm} \approx \frac{c_L^4}{32\sqrt{3}\ln^2(\pi/\varepsilon a_{vm})}\,\frac{\lambda}{\varepsilon}\,B_{vm}\Phi_\circ . \tag{22}$$

The various vortex phases and phase boundaries are illustrated in Fig. 1. The attraction between the vortices removes the dilute liquid phase at low temperatures, and the vortex system enters the specimen in a solid state. For highly layered materials the residual dilute gas phase is removed altogether as $T_g, T_{ve} \rightarrow T_c$, leading to a considerable simplification of the low-field phase diagram.

Experimental consequences of our new findings involve a first-order jump in the magnetization at H_{c_1} and the appearance of phase separation phenomena in the low-temperature regime. Besides a sufficiently strong anisotropy, a high sample quality (weak pinning) is required, with $Bi_2Sr_2Ca_1Cu_2O_8$ and $NbSe_2$ providing possible candidates.

We wish to thank E. H. Brandt, Ch. Bruder, M. P. A. Fisher, H. Katzgraber, D. R. Nelson, and A. van Otterlo for illuminating discussions.

[1] M. Tinkham, *Introduction to Superconductivity* (Krieger, Huntington, NY, 1980).
[2] E. H. Brandt, R. G. Mints, and I. B. Snapiro, Phys. Rev. Lett. **76**, 827 (1996).
[3] L. D. Landau and E. M. Lifshitz, *Course in Theoretical Physics* (Pergamon Press, London, 1958), Vols. 4 and 9.
[4] D. R. Nelson, Phys. Rev. Lett. **60**, 1973 (1988).
[5] G. Blatter *et al.*, Rev. Mod. Phys. **66**, 1125 (1994).
[6] I. S. Gradshteyn and I. M. Ryzhik, *Table of Integrals, Series, and Products* (Academic Press, New York, 1980).
[7] L. Xing and Z. Tešanović, Phys. Rev. Lett. **65**, 794 (1990).
[8] G. Blatter, V. Geshkenbein, A. Larkin, and H. Nordborg, Phys. Rev. B **54**, 72 (1996).